Cell Reports
Medicine

Article

A Small-Molecule Approach to Restore a Slow-Oxidative Phenotype and Defective CaMKIIβ Signaling in Limb Girdle Muscular Dystrophy

Graphical Abstract

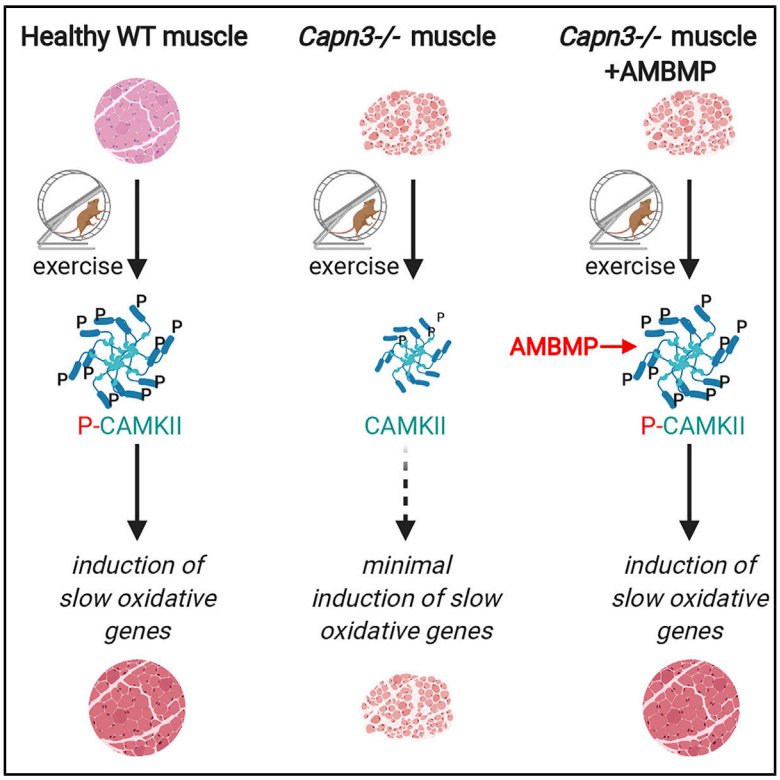

Highlights

- Exercise induces calcium calmodulin kinase activation and adaptive gene expression
- This signaling is blunted in *Capn3* deficiency, causing limb girdle muscular dystrophy
- A small molecule, AMBMP, is an exercise mimetic that induces these pathways
- AMBMP normalizes the *Capn3*$^{-/-}$ phenotype

Authors

Jian Liu, Jesus Campagna, Varghese John, ..., April D. Pyle, Irina Kramerova, Melissa J. Spencer

Correspondence

ikramero@ucla.edu (I.K.), mspencer@mednet.ucla.edu (M.J.S.)

In Brief

Failure to properly induce the signaling pathways that are activated by exercise and which promote the slow-oxidative gene expression program in muscle leads to limb girdle muscular dystrophy. Liu et al. report that a small molecule could activate these pathways and restore both the defective signaling and transcriptional patterns needed to reverse the muscle phenotype.

Liu et al., 2020, Cell Reports Medicine *1*, 100122
October 20, 2020
https://doi.org/10.1016/j.xcrm.2020.100122

CellPress

Cell Reports Medicine

CellPress
OPEN ACCESS

Article

A Small-Molecule Approach to Restore a Slow-Oxidative Phenotype and Defective CaMKIIβ Signaling in Limb Girdle Muscular Dystrophy

Jian Liu,[1,7] Jesus Campagna,[1] Varghese John,[1] Robert Damoiseaux,[2] Ekaterina Mokhonova,[1] Diana Becerra,[1] Huan Meng,[3] Elizabeth M. McNally,[6] April D. Pyle,[4,5] Irina Kramerova,[1,*] and Melissa J. Spencer[1,5,8,*]

[1]Department of Neurology, David Geffen School of Medicine at University of California, Los Angeles, Los Angeles, CA, USA
[2]Department of Pharmacology, David Geffen School of Medicine and Molecular Screening Shared Resource, Crump Imaging Institute, University of California, Los Angeles, Los Angeles, CA, USA
[3]Department of Medicine, David Geffen School of Medicine and California Nanosystems Institute, University of California, Los Angeles, Los Angeles, CA, USA
[4]Department of Microbiology, Immunology and Medical Genetics, David Geffen School of Medicine at University of California, Los Angeles, Los Angeles, CA, USA
[5]Eli and Edythe Broad Center of Regenerative Medicine and Stem Cell Research, University of California, Los Angeles, Los Angeles, CA, USA
[6]Center for Genetic Medicine, Northwestern University, Feinberg School of Medicine, Chicago, IL, USA
[7]Present address: Department of Biochemistry, University of Illinois, Urbana-Champaign, Champaign, IL, USA
[8]Lead Contact
*Correspondence: ikramero@ucla.edu (I.K.), mspencer@mednet.ucla.edu (M.J.S.)
https://doi.org/10.1016/j.xcrm.2020.100122

SUMMARY

Mutations in *CAPN3* cause limb girdle muscular dystrophy R1 (LGMDR1, formerly LGMD2A) and lead to progressive and debilitating muscle wasting. Calpain 3 deficiency is associated with impaired CaMKIIβ signaling and blunted transcriptional programs that encode the slow-oxidative muscle phenotype. We conducted a high-throughput screen on a target of CaMKII (*Myl2*) to identify compounds to override this signaling defect; 4 were tested *in vivo* in the *Capn3* knockout (C3KO) model of LGMDR1. The leading compound, AMBMP, showed good exposure and was able to reverse the LGMDR1 phenotype *in vivo*, including improved oxidative properties, increased slow fiber size, and enhanced exercise performance. AMBMP also activated CaMKIIβ signaling, but it did not alter other pathways known to be associated with muscle growth. Thus, AMBMP treatment activates CaMKII and metabolically reprograms skeletal muscle toward a slow muscle phenotype. These proof-of-concept studies lend support for an approach to the development of therapeutics for LGMDR1.

INTRODUCTION

Limb girdle muscular dystrophies (LGMDs) are genetically inherited, progressive muscle wasting diseases. LGMD2A is caused by mutations in the *CAPN3* gene. The disorder was initially described as an autosomal recessive disorder; however, new nomenclature reflects recently discovered autosomal dominant inheritance.[1–3] Thus, *CAPN3* mutations inherited in an autosomal recessive pattern are now referred to as LGMDR1, while those with autosomal dominant inheritance are referred to as LGMDD4. Both disorders appear to result in the loss of function of calpain 3 protease.

LGMDR1 patients usually present clinically in their second decade, demonstrating proximal muscle wasting and lacking cardiac or facial involvement.[4] Biopsies show fibers with disrupted myofibrillar architecture, small fiber diameter, and abnormal mitochondrial morphology and function.[5–8] Reduced sarcolemmal integrity is not a feature of LGMDR1, as is common in dystrophinopathies.[9]

To understand the pathogenic mechanisms of LGMDR1 and a role for Capn3 in skeletal muscle, we generated *Capn3* knockout (C3KO) mice.[10] Similar to LGMDR1 patients, these mice have reduced muscle fiber diameter, a mild but progressive dystrophy, and muscle weakness. Moreover, we found an association between the absence of Capn3 and reduced slow-oxidative (SO) fibers, dysfunctional mitochondria, and abnormal lipid metabolism.[11–13]

The changes described above may be related to the role of Capn3 in the maintenance of the integrity of the triad protein complex in skeletal muscle.[14] The triad is the site of calcium release that facilitates muscle contraction and which also initiates signaling pathways that elicit muscle remodeling in response to exercise.[15,16] The triad components RyR1 and calcium calmodulin kinase IIβ (CaMKIIβ) are both reduced in C3KO mice and in biopsies from LGMDR1 patients with null mutations.[12,14] CaMKIIβ reductions are associated with a dramatic decrease in overall CaMK levels and activation, while other isoforms of CaMK (α, γ, and δ isoforms) were not affected ([12,13,17

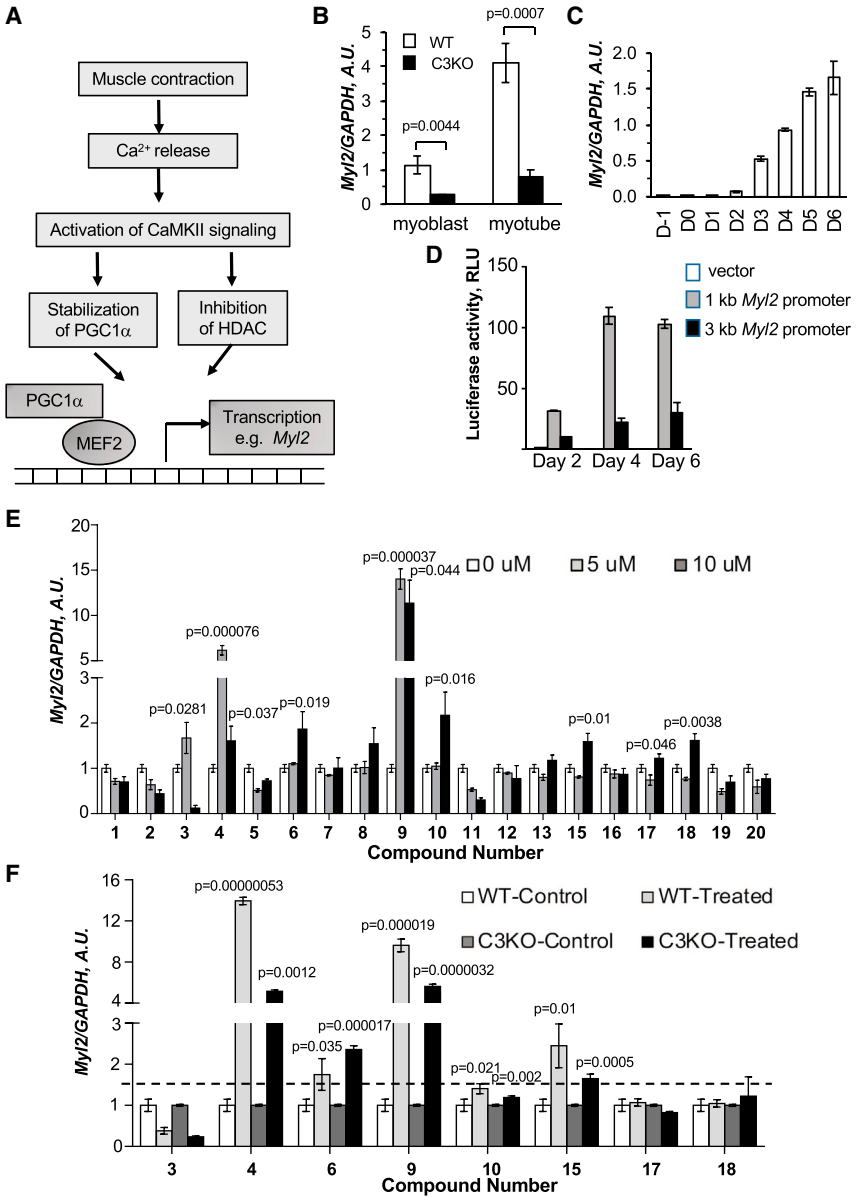

Figure 1. Development of a Myl2 Reporter System for HTS, and Identification of Compounds That Induce Endogenous Myl2 Expression

(A) Schematic representation of the CaMKII-mediated signaling pathways that regulate expression of downstream genes during muscle adaptation to loading, and which are defective in C3KO muscles. One such gene (*Myl2*) was used as a target in the screen.

(B) *Myl2* expression is induced in primary WT muscle cells during myogenic differentiation, but not induced in primary muscle cells isolated from C3KO muscles.

(C) *Myl2* expression linearly increases during C2C12 cell differentiation.

(D) Luciferase activities of both the 1- and 3-kb promoters increased during differentiation, but the 1-kb promoter had much higher activity than the 3-kb promoter.

(E) Graph of *Myl2* induction in C2C12 cells that were exposed to different concentrations of the top 20 compounds. Compounds were added during the initiation of differentiation, and after 48 h, cells were assessed for endogenous *Myl2* expression by RT-PCR. Compounds 3, 4, 6, 9, 10, 15, 17, and 18 were selected for further analysis in primary myogenic cells (in F).

(F) Assessment of endogenous *Myl2* expression in WT and C3KO primary cells after exposure to the top 8 compounds. *Myl2* was assessed by RT-PCR analysis. The following concentrations were used: 20 μM for number 6; 10 μM for numbers 17 and 18; 5 μM for numbers 3, 4, and 15; 2.5 μM for number 9; and 0.75 μM for number 10. Four compounds (4, 6, 9, and 15) increased endogenous *Myl2* expression by >1.5-fold and were thus selected for further testing *in vivo*. A.U., arbitrary units; RLU, relative luminometer units.

The vertical bars represent the standard error of the mean. The statistical analysis was performed using a Student's t test.

See also Table 1 and Figures S1 and S2.

and unpublished data). These changes in CaMKIIβ are post-translational, since neither the mRNA expression nor the splicing of CaMKIIβ were altered by the presence or absence of Capn3.[13]. Thus, the loss of Capn3 at the triad correlates with reduced triad components, reduced CaMKIIβ levels, and blunted CaMKIIβ signaling.

The concentration of CaMKIIβ at the triad enables it to serve a role as an exercise sensor. Furthermore, CaMKIIβ levels and activation increase with exercise in healthy muscles,[13,18–20] but this elevation does not occur in C3KO muscles, which instead show reduced CaMKIIβ levels at rest and no induction following exercise.[13] Blunted CaMKIIβ signaling in the absence of Capn3 correlated with a reduced percentage of slow fibers[12,13] and attenuated gene expression patterns in response to exercise. CaMKII-mediated signaling has been shown to act on two downstream pathways regulating muscle remodeling.[21] One pathway operates through the activation of p38, which in turn stabilizes PGC1α, a key transcriptional co-activator that orchestrates muscle adaptation responses.[22] PGC1α works in conjunction with several transcription factors such as peroxisome proliferator-activated receptors (PPARs) and myocyte enhancer factor-2 (MEF2) to regulate the transcription of metabolic and sarcomeric genes that are required for muscle adaptation. In addition, CaMKII also phosphorylates histone deacetylases (HDACs), allowing transcription of MEF2-mediated genes.[23,24] Among the genes controlled by the CaMKII-HDAC-MEF2 pathway is the slow isoform of myosin light chain (*Myl2*).[25]

A schematic representation of these pathways is shown in Figure 1A. We previously showed that both of the pathways downstream of CaMKII are blunted in C3KO mice,[12,13] thus compromising the ability of C3KO muscles to respond to changes in muscle contractile activity (e.g., exercise). As expected, we

observed the reduced expression of a set of genes encoding slow isoforms of sarcomeric proteins (including *Myl2*) and decreased transcripts of genes involved in oxidative metabolism in C3KO muscles.[13] The activation of other signaling pathways such as AKT or AMP kinase (AMPK) were not altered in the absence of Capn3 at rest nor after exercise.[9,13] Furthermore, we did not observe a reduction in calcineurin levels in C3KO muscles.[12] These data show that CaMKII-mediated signaling is specifically impaired in C3KO mice and that this defect results in the reduced expression of downstream genes required for muscle adaptation.

These observations, together with other findings in the mouse model of LGMDR1, suggest that the pathomechanisms underlying LGMDR1 are unique and that LGMDR1 patients are unlikely to benefit from the extensive drug development pipelines that are advancing for other muscular dystrophies. Because these patients have no treatment options, progress in therapeutics for LGMDR1 is a high priority.

To identify compounds to override the failed adaptive gene expression in LGMDR1, we conducted a high-throughput screen (HTS) on a target of CaMKIIβ (*Myl2* gene) and identified a small molecule that activates CaMKIIβ *in vivo* and improves the C3KO phenotype. The lead compound AMBMP (N^4-(1,3-benzodioxol-5-ylmethyl)-6-(3-methoxyphenyl)-2,4-pyrimidinediamine hydrochloride) can activate the expression of slow genes, improve the capacity for oxidative metabolism, and improve muscle function when administered to C3KO.

RESULTS

High-Throughput Screening on a CAMKIIβ Target (*Myl2*)

We previously showed a functional link between muscle activity, CaMKIIβ signaling, and subsequent transcription of SO genes. We observed that this pathway is blunted in C3KO muscles at rest and especially after exercise.[13] Figure 1A summarizes the pathways we identified as defective in C3KO muscle. Normally, prolonged muscle activity leads to the activation of CaMKII signaling, followed by the increased expression of genes required for muscle adaptation, particularly genes of the SO program. Both PGC1a levels and HDAC activity were reduced in C3KO, along with the transcription of genes encoding slow sarcomeric proteins and those involved in oxidative metabolism.[13] One such downstream gene is *Myl2*, which encodes the slow isoform of myosin light chain.[13] We chose to screen on Myl2 because (1) *Myl2* is induced along with other genes of the SO gene expression program[13] and (2) we observed a deficit in *Myl2* induction in C3KO with exercise, concomitant with the impaired activation of CaMKII.[12,13] Here, we show that *Myl2* expression is transcriptionally regulated in a linear fashion during differentiation in both wild-type primary cultures and an established myogenic cell line C2C12 (Figure 1C), but not induced in C3KO cells during the same differentiation protocol (Figure 1B). Thus, the *Myl2* gene was chosen as a marker of failed gene expression in C3KO and the *Myl2* promoter used to drive a luciferase reporter in a HTS.

Using our prior knowledge of the *Myl2* promoter,[26] we generated a *Myl2* promoter reporter construct that was subsequently used in an unbiased HTS on this CaMKIIβ signaling target. To identify compounds capable of activating *Myl2* expression, we cloned 1- or 3-kb fragments of the *Myl2* promoter into a firefly luciferase reporter vector pGL4.17.

C2C12 cells were transfected with these reporter constructs and then further tested to determine whether the luciferase activity reflected endogenous *Myl2* gene expression. As shown in Figure 1D, luciferase reporter activity increased during differentiation, although activity from the 1-kb promoter was significantly higher than activity from the 3-kb promoter, suggesting the presence of a repressor in the upstream region of the promoter. In contrast, only low levels of activity were detected in cells transfected with a control vector (promoterless luciferase pGL4.17).

For the HTS, we screened on both the 1- and 3-kb *Myl2*-reporter constructs, after generating stably transfected C2C12 cells. Although the activity of the 3-kb promoter was much lower than the 1-kb promoter, we decided to screen on both promoters. The rationale for screening the 3-kb promoter is because we observed HDAC nuclear retention in C3KO, which leads to transcriptional repression.[12] Thus, we reasoned that the 3-kb promoter may be a good model of transcriptional repression.

Using stably transfected C2C12 cells, we screened the LOPAC and Prestwick small-molecule libraries. The LOPAC library comprises 1,028 pharmacologically active and US Food and Drug Administration (FDA)-approved compounds. The Prestwick library comprises 1,028 approved drugs. In the initial screen, all of the compounds were added to the cells at a 10-μM final concentration in DMSO. Primary hits were defined as compounds that produced an increase in luciferase activity of >3 standard deviations over vehicle (DMSO) control wells (Z score = 3). In the initial screen, we identified 33 hits from the 1-kb *Myl2*-reporter cells and 30 hits from the 3-kb *Myl2*-reporter cells (Table S1). These molecules had diverse but overlapping mechanisms of action that included Wnt signaling, glucocorticoids, proton pump inhibitor, non-steroidal anti-inflammatory drugs, and carbonic anhydrase inhibitors. All 58 hits from the initial screen were further tested in triplicate, and 20 compounds were retained for further evaluation (Table 1). All 20 compounds activated *Myl2* in cells stably expressing both the 1- and 3-kb promoters.

The dose response of the top 20 hits was assessed and revealed that 16 of 20 compounds showed a concentration-dependent activation of the reporter (Figure S1). We also performed cytotoxicity and cell viability assays at a wide concentration range (up to 100 μM) for these 20 compounds (Figure S2).

Next, we tested the effect of the 20 validated hits on endogenous *Myl2* expression in C2C12 cells using 2 different doses (5 and 10 μM). Real-time PCR analysis showed that 8 compounds could significantly increase endogenous *Myl2* expression in C2C12 cells (Figure 1E). Among those, compounds 4 and 9 were the most potent. We next assessed whether the top 8 compounds could activate endogenous *Myl2* in primary myogenic cells derived from wild-type (WT) and C3KO muscles (Figure 1F) and identified 4 compounds (numbers 4, 6, 9, and 15) that increased *Myl2* expression by ≥1.5-fold. We also tested whether these same compounds could activate other genes of the SO program (e.g., *Ckmt2, Pnpla2*), which we previously

Table 1. List of Top 20 Validated Compounds from Primary HTS Obtained from Screen on Both the 1- and 3-kb Promoters

No.	Compound name	Known function
1	6-methyl-2-(phenylethynyl) pyridine hydrochloride	antagonist of mGlu5 metabotropic glutamate receptor
2	apomorphine hydrochloride hemihydrate	nonselective dopamine agonist
3	BIO	GSK-3α/β inhibitor
4	AMBMP	activator of Wnt signaling without inhibiting GSK-3β
5	daidzein	inhibitor of mitochondrial aldehyde dehydrogenase
6	lansoprazole	gastric proton pump inhibitor
7	nabumetone	NSAIDs
8	olomoucine	NSAIDs
9	parbendazole	broad-spectrum anthelmintic activity
10	PD-98059	inhibitor of MAPKK
11	phenamil methanesulfonate salt	irreversible inhibitor of amiloride-sensitive Na^+ channels
12	phenazopyridine hydrochloride	analgesic drug
13	phenelzine sulfate	potent inhibitor of MAO
14	quinacrine Dihydrochloride Dihydrate	phospholipase A2 inhibitor
15	rabeprazole sodium salt	gastric H^+/K^+ ATPase pump inhibitor
16	rutaecarpine	delayed rectifier K^+ channel blocker
17	SB 204741	5-HT2B serotonin receptor antagonist
18	SB-206553 hydrochloride hydrate	5-HT2C/5-HT2B serotonin receptor antagonist
19	SB-366791	selective TRPV1 antagonist
20	SIB 1893	antagonist of mGlu5 metabotropic glutamate receptor

FDA-approved compounds include lansoprazole, nabumetone, phenazopyridine hydrochloride, phenelzine sulfate, quinacrine dihydrochloride dihydrate, and rabeprazole sodium salt. FDA, US Food and Drug Administration; GSK-3α/β, glycogen synthase kinase 3 α/β; HTS, high-throughput screen; MAO, monoamine oxidase; MAPKK, mitogen-activated protein kinase kinase; NSAIDs, non-steroidal anti-inflammatory drugs; TRPV1, transient receptor potential vanilloid type 1.

identified as repressed in our C3KO model.[13] Based on these results, compounds 4, 6, 9, and 15 (AMBMP, lansoprazole, parbendazole, and rabeprazole, respectively) emerged as the 4 lead candidates. Interestingly, 3 of the 4 compounds are proton pump inhibitors (lansoprazole, parbendazole, and rabeprazole).

Assessment of the Top Four Candidates *In Vivo*

AMBMP, lansoprazole, parbendazole, and rabeprazole were subsequently tested *in vivo* after 2 weeks of daily intraperitoneal (i.p.) injections, followed by the assessment of *Myl2* and *Ckmt2* gene expression by RT-PCR. One compound, AMBMP, boosted both *Myl2* and *Ckmt2* expression *in vivo* (Figures 2A and 2B). Pharmacokinetic (PK) assessment of the four compounds revealed that the three proton pump inhibitors had poor exposure after *in vivo* administration. None were detected in blood after 2 h (data not shown). We assessed PK after oral gavage, intrapertioneal (i.p.) injection, subcutaneous (s.c.) injection, and in food at 2 dosages (10 and 30 mg/kg). After drug administration, blood was collected at 0.5, 1, 2, 4, and 6 h post-dose. The area under the curve (AUC) and C_{max} were calculated for each route of delivery. As shown in Figures 2C and 2D, s.c. and i.p. administration resulted in significantly higher C_{max} and AUC compared to the oral routes of delivery. We also examined the levels of AMBMP in skeletal muscles after systemic administration (i.p. injection) using high-performance liquid chromatography-mass spectrometry (HPLC-MS) analysis. As shown in Figure S3, AMBMP was detected in skeletal muscle and its concentration was stable up to 4 h post-injection. Based on these data, AMBMP emerged as our lead candidate for proof of concept testing *in vivo*.

The chemical structure of AMBMP is shown in Figure 2E and its pharmacological characteristics such as dose response, effects on cell viability, and toxicity are shown in Figure 2G (see Figure S1 for the dose response of all 20 compounds). More important, AMBMP is not only able to activate *Myl2* but it also activates other genes associated with the SO phenotype (Figure 2F). These genes are coordinately regulated in response to exercise in WT mice but not in C3KO mice.[13] These data validate AMBMP as our lead candidate for further proof of concept studies *in vivo* using C3KO mice as a LGMDR1 model.

AMBMP Can Ameliorate Phenotypic Features of Capn3-Deficient Muscles

We next tested the ability of AMBMP to improve the phenotype of our murine model of LGMDR1, as proof of concept for our approach. C3KO mice were treated with AMBMP for 2 weeks, receiving daily doses ranging from 3 to 30 mg/kg and administered via s.c. and i.p. routes of delivery, based on the results of preliminary PK and efficacy testing. AMBMP treatment at 7.5–15.0 mg/kg (i.p.) was most efficacious, based on fiber type and fiber size measurements. Cage-side observations did not reveal any obvious toxicity (e.g., weight loss, loss of grooming, loss of activity) in mice treated for 2 weeks with AMBMP (Figure S4). We did not observe cardiac hypertrophy (Figure S5). In addition, histological evaluation of skeletal muscles and heart did not reveal any obvious pathological changes such as fibrosis or inflammation (Figures S5 and S6).

A reduction in the SO phenotype is a characteristic feature of LGMDR1, including qualities such as reduced mitochondrial function and impaired oxidative metabolism.[8,12,13] Two weeks of AMBMP treatment (7.5 or 15 mg/kg daily i.p. administration) led to significant improvements in the SO properties of C3KO muscles. We observed an increased number of oxidative fibers, as assessed by NADH stain (Figures 3A, 3B, and S6). Slow myosin heavy-chain staining revealed a trend toward an increase in the percentage of slow myosin,

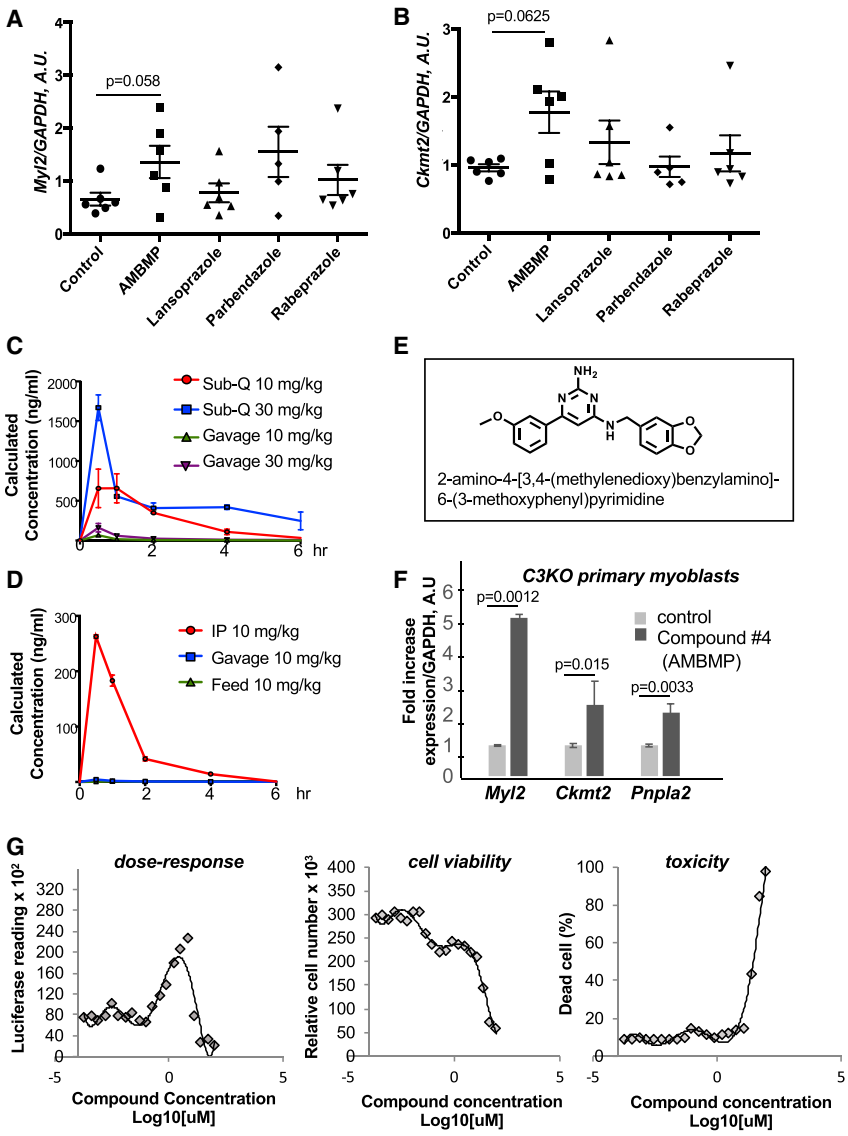

Figure 2. *In Vivo* Testing of the 4 Lead Compounds and Identification of AMBMP as the Lead Candidate

(A and B) The top 4 compounds were administered to WT mice for 2 weeks by daily intraperitoneal (i.p.) injection. The dosing was as follows: AMBMP (7.5 mg/kg), lansoprazole (10 mg/kg), rabeprazole (30 mg/kg), and parbendazole (11.27 mg/kg). Plantaris muscles were assessed for *Myl2* (A) and *Ckmt2* (B) levels by RT-PCR. N = 6/group, age = 5–8 months old. Each dot represents data from 1 mouse. The vertical bars represent the standard error of the mean;

(C and D) Pharmacokinetic analysis of AMBMP. WT mice were administered AMBMP by subcutaneous injection (s.c.) or oral delivery in dosing of 10 and 30 mg/kg (C), or by i.p. injection, gavage, or incorporated into the food in doses of 10 mg/kg (D). Plasma was collected at 0.5, 1, 2, 4, and 6 h post-treatment and was tested for AMBMP concentration.

(E) Chemical structure of AMBMP

(F) RT-PCR analysis of *Myl2, Ckmt2*, and *Pnpla2* gene expression in C3KO primary muscle cells treated with 5 μM AMBMP. These genes were chosen because they are improperly regulated in C3KO muscles.

(G) Dose response, cell viability, and toxicity were assessed using a 20-point titration of AMBMP in stably transfected (1 kb promoter) C2C12 cells.

The vertical bars represent the standard error of the mean. The statistical analysis was performed with Student's t test for 2 group comparisons (F) and 1-way ANOVA for multiple comparisons (A and B) with Tukey's post hoc test.

See also Figure S3.

but the data were not significantly different at this dosage and route of administration (Figure 3C). Moreover, AMBMP-treated muscles showed significant improvements in mitochondrial respiration, as assessed by the XF96 Seahorse Extracellular Flux Analyzer. Both mitochondrial complex I (39%) and complex II (36%) activities increased after 2 weeks of drug treatment (Figure 3D). AMBMP improved the muscle fiber cross-sectional area (CSA) of slow fibers in the soleus muscle (Figure 3E), but it did not significantly increase the CSA of fast fibers (although a trend toward increase was observed) (Figure 3F).

Consistent with the improvements in the oxidative phenotype and increased muscle fiber size, AMBMP also improved exercise performance. We showed previously (and shown in Figure 4A) that C3KO mice perform significantly worse than WT mice in a treadmill run to exhaustion test[13]. However, C3KO mice treated daily with 7.5 mg/kg AMBMP by i.p. administration for 14 days showed a significant increase in exercise performance over vehicle-treated mice by 30% (Figure 4B). Thus, AMBMP treatment led to improvements in oxidative metabolism, oxidative fiber CSA, and endurance exercise performance in C3KO mice, thus reversing phenotypic features of disease.

AMBMP Targets CaMKIIβ *In Vivo*

We next asked whether AMBMP acts by enhancing CaMKIIβ activity *in vivo*. C3KO and C57BL/6 WT mice were treated with AMBMP and then their muscles were evaluated for CaMKIIβ and other signaling pathways. The activation of signaling was carried out by western blotting with antibodies specific for the active forms of these signaling pathways. Treatment with AMBMP (daily i.p. injection 7.5 mg/kg) led to CaMKIIβ activation in both WT and C3KO mice (Figures 4C and 4D). The drug appears to engage CaMKIIβ specifically as it does not activate AKT nor AMPK (nor other pathways that control muscle remodeling and oxidative metabolism) (Figures 4E and 4F). Furthermore, the effect of AMBMP on CaMKIIβ was likely post-transcriptional, and there was no significant change in the

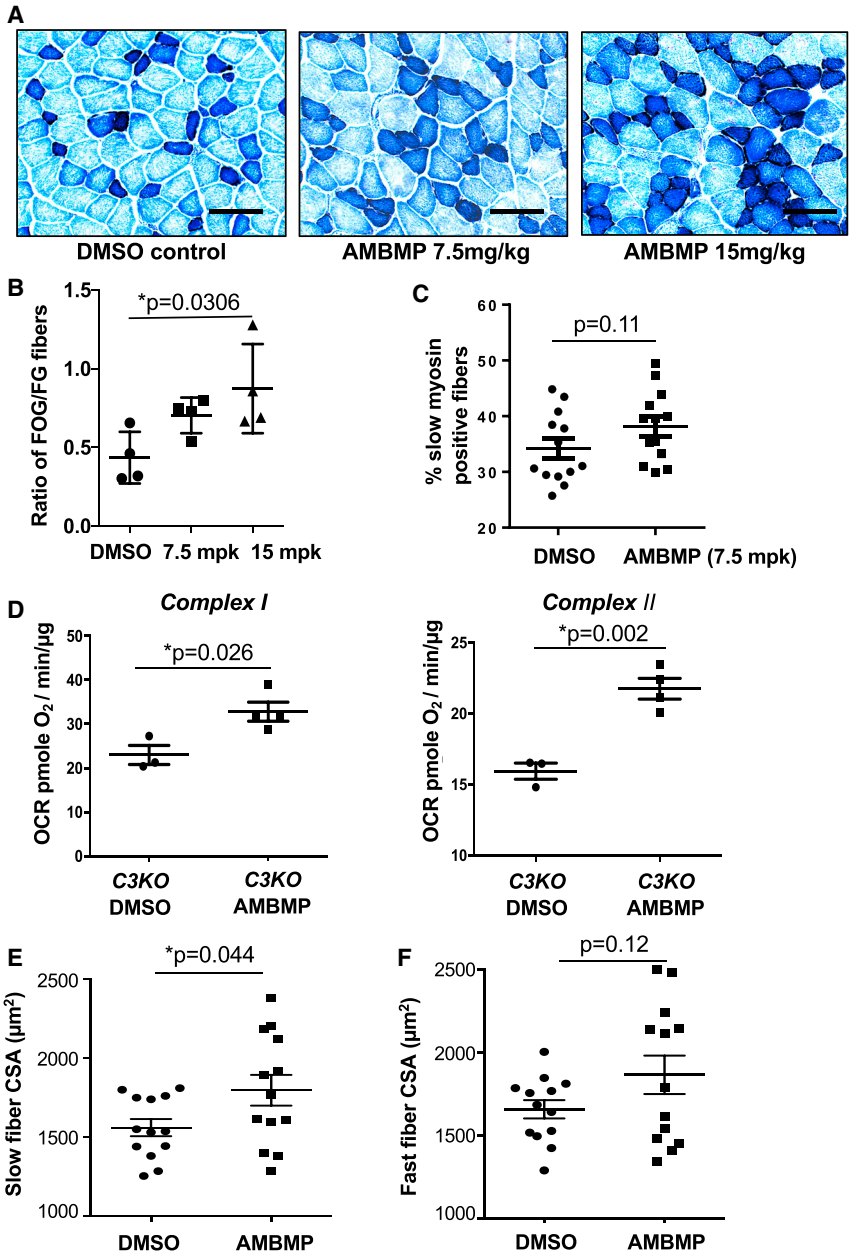

Figure 3. Proof of concept that AMBMP Treatment Improves the Oxidative Capacity of Calpain 3-Deficient Muscles

(A) NADH-stained cross-sections of C3KO plantaris muscles from mice treated with DMSO or with 2 different concentrations of AMBMP; scale bar, 100 μm. The darker color reflects increased slow-oxidative fibers.

(B) Quantification of (A) in which the ratio of fast-oxidative/glycolytic (FOG) to fast-glycolytic (FG) fibers was determined.

(C) Percentage of fibers expressing slow myosin heavy chain (sMHC), quantified from sections of soleus muscles from mice treated with DMSO or AMBMP (7.5 mg/kg i.p.) after immunostaining for sMHC.

(D) Seahorse analysis of complex I and complex II activities in muscles from mice treated for 2 weeks with either DMSO or 7.5 mg/kg AMBMP.

(E and F) Average cross-sectional area (CSA) of (E) slow and (F) fast fibers from AMBMP- or DMSO-treated C3KO mouse solei. Sections were stained with slow myosin heavy chain before the assessment of CSA so that slow and fast fibers could be assessed independently. C3KO mice were i.p. injected with AMBMP (7.5 mg/kg/day) for 14 days. Whole-muscle cross-sections were analyzed. Each dot represents the data from 1 mouse.

The vertical bars represent the standard error of the mean. The statistical analysis was performed with a Student's t test for 2 group comparisons (C–F) and 1-way ANOVA for multiple comparisons (B) with Tukey's post hoc test.

See also Figures S4–S6.

expression level of the *Camk2b* gene (Figure 4G). Thus, these studies establish proof of concept for the ability of AMBMP to activate CaMKII and subsequently to promote oxidative metabolism and benefit the LGMDR1 phenotype.

DISCUSSION

In the present study, we conducted a HTS on a CaMKIIβ target of the SO program (*Myl2*)[13] to identify compounds to treat LGMDR1/D4. We initially identified and validated 20 compounds from our screen. Secondary screening narrowed our focus to AMBMP, which was later extensively tested *in vitro* and *in vivo* which provided support for our hypothesis that bunted CaMK signaling can be over-riden using a small molecule approachWe have now demonstrated proof of concept that this approach can lead to new small molecules capable of activating CaMKIIβ and improving the oxidative and functional properties of Capn3-deficient muscles *in vivo*.

LGMDR1 is caused by loss of function mutations in *CAPN3*[27] and is believed to be the most prevalent of the known LGMDs.[28] Our work has revealed a remodeling defect in Capn3-deficient muscles, which was uncovered using experimental protocols that induce atrophy and growth (hindlimb unloading/reloading) or following exercise training.[9,12,13,17] Deconditioning occurs because muscles lacking Capn3 do not sense loading and do not activate the signaling pathways (especially CaMKII) necessary to maintain the SO gene transcription program. Long-term downregulation of the SO program results in the severe loss of muscle bulk and the inability of weakened muscles to support body mass, leading to muscle cell death. We posit that failure to activate these remodeling pathways underlies disease in LGMDR1.

Failure to maintain the SO program in LGMDR1 is due to insufficient CaMKIIβ signaling, which is a pathway normally initiated by muscle use. The CaMKIIβ signaling defect is caused by the

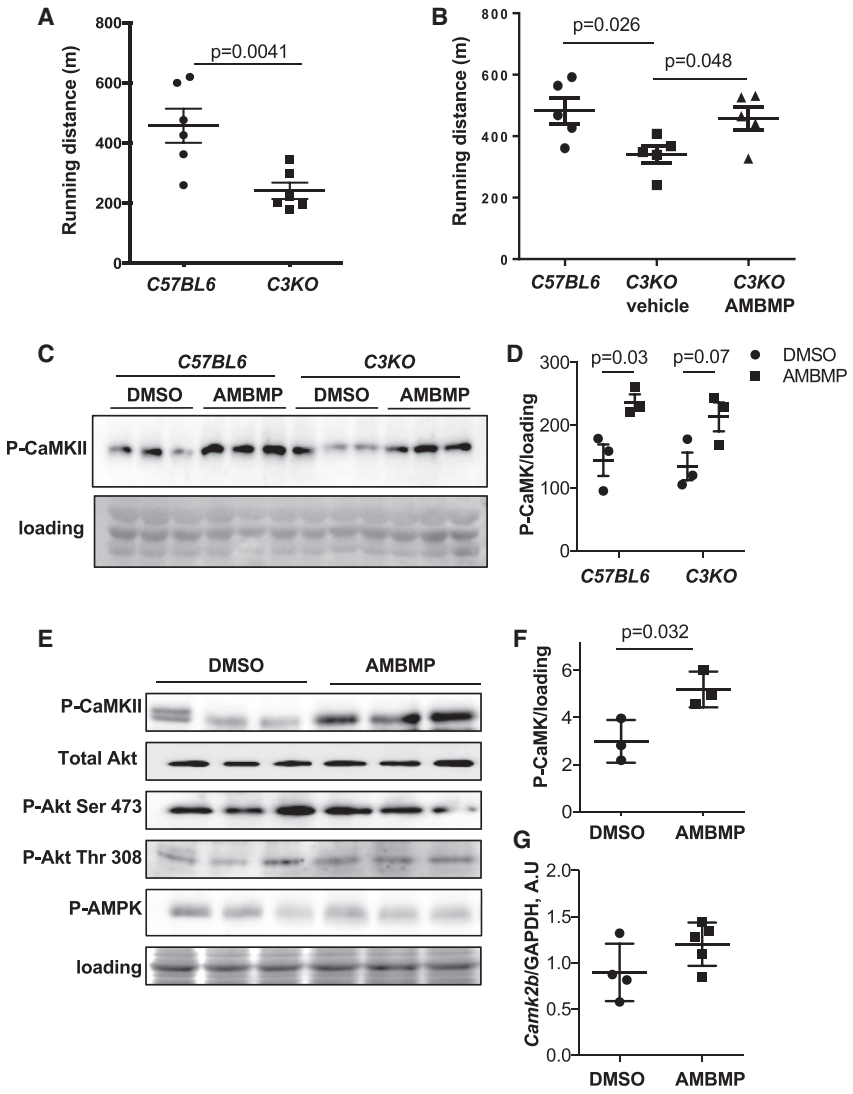

Figure 4. AMBMP Treatment Activates CaMKIIβ Signaling and Improves Exercise Performance

(A) C3KO mice show impaired running performance compared to C57Bl6 WT mice.

(B) C3KO mice treated with daily 7.5 mg/kg AMBMP for 14 days improved their running performance compared to untreated C3KO. Each dot represents the data from 1 mouse. WT mice were not treated with the drug.

(C and D) Western blot analysis of phospho-CaMKIIβ in plantaris from WT and C3KO mice (treated with either DMSO or 2 weeks of daily AMBMP at 7.5 mg/kg) (C). Quantification of the signal intensity is shown in (D).

(E and F) AMBMP treatment activates CaMKIIβ, but does not activate AKT or AMPK signaling under the same dosing regimen (E). Quantification of the signal intensity of the CaMKII blot (top blot in E) is shown in (F).

(G) Real-time PCR analysis of *Camk2b* gene expression after 2 weeks of daily AMBMP (7.5 mg/kg).

The vertical bars represent the standard error of the mean. The statistical analysis was performed with a Student's t test for 2 group comparisons (A, D, F, and G) and 1-way ANOVA with Tukey's post hoc analysis (B).

failure to retain CaMKIIβ in the triad complex, due to the absence of Capn3.[14,29,30] Maintaining CaMKIIβ at a site of high Ca release allows it to serve as an exercise sensor to promote downstream transcriptional programs. Loss of Capn3 also leads to overall reductions in (1) CaMKIIβ levels, (2) activated CaMKIIβ, and (3) subsequent failure to increase the transcription of downstream target genes.[13,17] Blunted CaMKIIβ signaling represents a disease mechanism that is distinct from other muscular dystrophies; however, we anticipate that the decreased activation of this pathway could contribute to the loss of muscle remodeling in many other contexts. For example, when patients are wheelchair restricted or confined to bed, they experience disuse atrophy. The lack of loading that accompanies these states would likely lead to reduced signals to activate CaMKIIβ and further exacerbate muscle wasting. Furthermore, there are several genetically inherited myopathies that are linked to triad proteins (i.e., triadopathies)[31] that could benefit from a drug such as AMBMP. Most important, our studies reveal that CaMKIIβ signaling and downstream activation of gene expression is vital for the maintenance of muscle health.

AMBMP has been used in prior research studies as a Wnt agonist,[32,33] although the mechanism by which AMBMP affects Wnt signaling is not clear. Wnts are a family of signaling molecules that activate canonical or noncanonical pathways.[34] The best-known function of the Wnt canonical pathway is the induction of cell proliferation, but it is highly unlikely that AMBMP is acting in this manner to affect the C3KO phenotype, since muscle is post-mitotic. In addition, we did not see an increase in muscle regeneration (based on developmental myosin heavy-chain staining), which is the consequence of muscle stem cell activation, suggesting that the actions of AMBMP on skeletal muscle are unrelated to either cell proliferation or promotion of regeneration.

Our studies demonstrate that AMBMP activates CaMKII signaling, which is a pathway that is impaired in C3KO mice. It is still unclear whether reduced Wnt signaling is fundamental to the failure to activate CaMK. One study has suggested that Wnt signaling is abnormal in LGMDR1 muscles due to the overexpression of Wnt antagonist FRZB,[35] but how those studies relate to our findings is unclear. Interestingly, several Wnt family members have been shown to stimulate the release of intracellular Ca, probably via heterotrimeric G proteins, to activate downstream phospholipase C (PLC), protein kinase C (PKC) and CaMKII.[34,36,37] It is possible that this increased intracellular Ca may be responsible for the supplementary activation of the

CaMKII pathway, thus overriding the defects that we identified in Capn3-deficient mice.

The function of Wnt/Ca^{2+} signaling in skeletal muscle has not been well studied. Canonical Wnt signaling plays an important role during embryonic skeletal muscle development by controlling the expression of key myogenic regulatory factors (MRFs).[38] In adult muscle, Wnt signaling is required for muscle regeneration after injury, as well as for self-renewal of muscle stem cells to prevent their depletion.[38] Given the important role of muscle stem cells in myogenesis and in adult skeletal muscle homeostasis, Wnt proteins have been proposed to represent promising therapeutic candidates for muscular dystrophies. For example, Wnt7a has been shown to activate the AKT/mammalian target of rapamycin (mTOR) pathway in skeletal muscle, leading to muscle hypertrophy and improved force generation.[39] The treatment of mdx mice (a model for Duchenne muscular dystrophy) with Wnt7a led to muscle stem cell expansion, myofiber hypertrophy, and increased muscle strength.[40] Interestingly, treatment with Wnt7a resulted in a fiber-type shift toward more slow twitch fibers.[40] In our study, we did not see an effect of AMBMP on AKT or AMPK signaling; however, our data showed that it increased the SO phenotype, as evidenced by increased slow fibers, increased oxidative fibers, and improved mitochondrial function.

AMBMP is toxic to cells at high concentrations *in vitro*, due to its microtubule binding activity.[41] We also observed similar toxicity *in vitro*, but this finding did not translate to the *in vivo* setting. Similarly, AMBMP has been used as a Wnt agonist in several *in vivo* studies without toxicity.[32,42,43] In our experiments, we were able to treat mice for 2 weeks with AMBMP without adverse signs in skeletal muscles or heart (Figures S4–S6). Nevertheless, to further improve the efficacy of AMBMP for translation, we are designing new chemical analogs of AMBMP to improve its solubility, safety, and drug-like properties.

The findings here show that the C3KO phenotype is reversible through the activation of CaMKIIβ. Our data also support our initial hypothesis that defects in CaMKIIβ signaling underlie the pathogenesis of LGMDR1 and that this pathway plays an important role in skeletal muscle remodeling. It is feasible that CaMKIIβ signaling is commonly downregulated in the muscles of individuals with reduced mobility of any sort, and thus, AMBMP is an exercise mimetic that could be widely useful for improving muscle health in a variety of contexts. This study supports CaMKII signaling as a valid therapeutic target for LGMDR1.

Limitations of Study

The mouse model used in this study has some limitations. The *Capn3*$^{-/-}$ mouse[10] is a genetic homolog of LGMDR1 patients that have null mutations, and the mouse replicates many features of disease, such as abnormal mitochondria,[8,11] small fiber diameter,[44] muscle weakness,[13] and muscle degeneration.[10] However, the *Capn3*$^{-/-}$ mouse is lacking the fibrosis observed in LGMDR1 biopsies.[45] The lack of fibrosis likely reflects the milder disease course that is observed in the mouse versus human. Furthermore, although the *Capn3*$^{-/-}$ mouse is a genetic homolog to patients carrying two null mutations, many patients are compound heterozygotes—they harbor either one missense and one null mutation or two missense mutations. Thus, it is possible that these studies in the *Capn3*$^{-/-}$ model do not fully recapitulate the biochemical and phenotypic features of patients with missense mutations.

STAR★METHODS

Detailed methods are provided in the online version of this paper and include the following:

- KEY RESOURCES TABLE
- RESOURCE AVAILABILITY
  - Lead Contact
  - Materials Availability
  - Data and Code Availability
- EXPERIMENTAL MODEL AND SUBJECT DETAILS
  - Mouse Models
  - Cell lines used
- METHOD DETAILS
  - Animal studies
  - Treatment of C2C12 cells
  - Cloning of Myl2 promoter reporter constructs and generation of C2C12 stable cell lines
  - High throughput and secondary screening
  - Compound dose response analysis
  - Cytotoxicity and viability assay
  - Compound treatment of C2C12 cells
  - Isolation and compound treatment of primary myoblasts
  - Real-time PCR
  - Compound pharmacokinetics assay
  - Quantification of cross-sectional area and NADH staining
  - Seahorse analysis of Extracts from Frozen Muscle
  - Western blot analysis
  - Statistical analysis

SUPPLEMENTAL INFORMATION

Supplemental Information can be found online at https://doi.org/10.1016/j.xcrm.2020.100122.

ACKNOWLEDGMENTS

This work was largely supported through a generous donation from the MyDirectives Universal Advance Digital Directive. In addition, the work was funded by the National Institute of Arthritis and Musculoskeletal and Skin Diseases through a Wellstone Cooperative Muscular Dystrophy Center (U54AR052646) and a P30 Muscular Dystrophy Core Center (NIAMS-P30AR057230), as well as through the NIH National Center for Advancing Translational Science (NCATS) UCLA CTSI grant no. UL1TR001881 (seed grant) and support from Strongbridge Biopharma. The authors would like to thank Ms. Jane Wen for technical support and Dr. Ellen Welch, Mr. Jeff Zucker, and Mr. Bhulo Kansagra for helpful discussions.

AUTHOR CONTRIBUTIONS

Conceptualization, M.J.S. and I.K. Methodology, M.J.S., J.L., I.K., V.J., and R.D. Investigation, J.L., J.C., E.M., D.B., and I.K. Writing – Original Draft, J.L., I.K., and M.J.S. Writing – Review & Editing, M.J.S., I.K., E.M.M., A.D.P.,

H.M., and V.J. Funding Acquisition, M.J.S., I.K., and V.J. Resources, R.D. Supervision, M.J.S., I.K., and V.J.

DECLARATION OF INTERESTS

M.J.S. and A.D.P. are co-founders of MyoGene Bio and are members of its scientific advisory board. M.J.S., I.K., J.C., and V.J. are inventors on a patent pending pertaining to new chemical entities of AMBMP.

Received: December 14, 2019
Revised: August 7, 2020
Accepted: September 21, 2020
Published: October 7, 2020

REFERENCES

1. Straub, V., Murphy, A., and Udd, B.; LGMD Workshop Study Group (2018). 229th ENMC international workshop: limb girdle muscular dystrophies - nomenclature and reformed classification Naarden, the Netherlands, 17-19 March 2017. Neuromuscul. Disord. *28*, 702–710.
2. Taghizadeh, E., Rezaee, M., Barreto, G.E., and Sahebkar, A. (2019). Prevalence, pathological mechanisms, and genetic basis of limb-girdle muscular dystrophies: a review. J. Cell. Physiol. *234*, 7874–7884.
3. Vissing, J., Barresi, R., Witting, N., Van Ghelue, M., Gammelgaard, L., Bindoff, L.A., Straub, V., Lochmüller, H., Hudson, J., Wahl, C.M., et al. (2016). A heterozygous 21-bp deletion in CAPN3 causes dominantly inherited limb girdle muscular dystrophy. Brain *139*, 2154–2163.
4. Richard, I., Hogrel, J.Y., Stockholm, D., Payan, C.A., Fougerousse, F., Eymard, B., Mignard, C., Lopez de Munain, A., Fardeau, M., and Urtizberea, J.A.; Calpainopathy Study Group (2016). Natural history of LGMD2A for delineating outcome measures in clinical trials. Ann. Clin. Transl. Neurol. *3*, 248–265.
5. Fanin, M., Nascimbeni, A.C., and Angelini, C. (2013). Muscle atrophy in Limb Girdle Muscular Dystrophy 2A: a morphometric and molecular study. Neuropathol. Appl. Neurobiol. *39*, 762–771.
6. Fanin, M., and Angelini, C. (2015). Protein and genetic diagnosis of limb girdle muscular dystrophy type 2A: The yield and the pitfalls. Muscle Nerve *52*, 163–173.
7. Guglieri, M., Magri, F., D'Angelo, M.G., Prelle, A., Morandi, L., Rodolico, C., Cagliani, R., Mora, M., Fortunato, F., Bordoni, A., et al. (2008). Clinical, molecular, and protein correlations in a large sample of genetically diagnosed Italian limb girdle muscular dystrophy patients. Hum. Mutat. *29*, 258–266.
8. El-Khoury, R., Traboulsi, S., Hamad, T., Lamaa, M., Sawaya, R., and Ahdab-Barmada, M. (2019). Divergent Features of Mitochondrial Deficiencies in LGMD2A Associated With Novel Calpain-3 Mutations. J. Neuropathol. Exp. Neurol. *78*, 88–98.
9. Kramerova, I., Kudryashova, E., Venkatraman, G., and Spencer, M.J. (2005). Calpain 3 participates in sarcomere remodeling by acting upstream of the ubiquitin-proteasome pathway. Hum. Mol. Genet. *14*, 2125–2134.
10. Kramerova, I., Kudryashova, E., Tidball, J.G., and Spencer, M.J. (2004). Null mutation of calpain 3 (p94) in mice causes abnormal sarcomere formation in vivo and in vitro. Hum. Mol. Genet. *13*, 1373–1388.
11. Kramerova, I., Kudryashova, E., Wu, B., Germain, S., Vandenborne, K., Romain, N., Haller, R.G., Verity, M.A., and Spencer, M.J. (2009). Mitochondrial abnormalities, energy deficit and oxidative stress are features of calpain 3 deficiency in skeletal muscle. Hum. Mol. Genet. *18*, 3194–3205.
12. Kramerova, I., Kudryashova, E., Ermolova, N., Saenz, A., Jaka, O., López de Munain, A., and Spencer, M.J. (2012). Impaired calcium calmodulin kinase signaling and muscle adaptation response in the absence of calpain 3. Hum. Mol. Genet. *21*, 3193–3204.
13. Kramerova, I., Ermolova, N., Eskin, A., Hevener, A., Quehenberger, O., Armando, A.M., Haller, R., Romain, N., Nelson, S.F., and Spencer, M.J. (2016). Failure to up-regulate transcription of genes necessary for muscle adaptation underlies limb girdle muscular dystrophy 2A (calpainopathy). Hum. Mol. Genet. *25*, 2194–2207.
14. Kramerova, I., Kudryashova, E., Wu, B., Ottenheijm, C., Granzier, H., and Spencer, M.J. (2008). Novel role of calpain-3 in the triad-associated protein complex regulating calcium release in skeletal muscle. Hum. Mol. Genet. *17*, 3271–3280.
15. Franzini-Armstrong, C., and Jorgensen, A.O. (1994). Structure and development of E-C coupling units in skeletal muscle. Annu. Rev. Physiol. *56*, 509–534.
16. Chin, E.R. (2005). Role of Ca2+/calmodulin-dependent kinases in skeletal muscle plasticity. J. Appl. Physiol. (1985) *99*, 414–423.
17. Kramerova, I., Torres, J.A., Eskin, A., Nelson, S.F., and Spencer, M.J. (2018). Calpain 3 and CaMKIIβ signaling are required to induce HSP70 necessary for adaptive muscle growth after atrophy. Hum. Mol. Genet. *27*, 1642–1653.
18. Combes, A., Dekerle, J., Webborn, N., Watt, P., Bougault, V., and Daussin, F.N. (2015). Exercise-induced metabolic fluctuations influence AMPK, p38-MAPK and CaMKII phosphorylation in human skeletal muscle. Physiol. Rep. *3*, e12462.
19. Rose, A.J., and Hargreaves, M. (2003). Exercise increases Ca2+-calmodulin-dependent protein kinase II activity in human skeletal muscle. J. Physiol. *553*, 303–309.
20. Rose, A.J., Frøsig, C., Kiens, B., Wojtaszewski, J.F., and Richter, E.A. (2007). Effect of endurance exercise training on Ca2+ calmodulin-dependent protein kinase II expression and signalling in skeletal muscle of humans. J. Physiol. *583*, 785–795.
21. Hoppeler, H. (2016). Molecular networks in skeletal muscle plasticity. J. Exp. Biol. *219*, 205–213.
22. Olesen, J., Kiilerich, K., and Pilegaard, H. (2010). PGC-1alpha-mediated adaptations in skeletal muscle. Pflugers Arch. *460*, 153–162.
23. Potthoff, M.J., and Olson, E.N. (2007). MEF2: a central regulator of diverse developmental programs. Development *134*, 4131–4140.
24. Duran, J., Lagos, D., Pavez, M., Troncoso, M.F., Ramos, S., Barrientos, G., Ibarra, C., Lavandero, S., and Estrada, M. (2017). Ca2+/Calmodulin-Dependent Protein Kinase II and Androgen Signaling Pathways Modulate MEF2 Activity in Testosterone-Induced Cardiac Myocyte Hypertrophy. Front. Pharmacol. *8*, 604.
25. Sandmann, T., Jensen, L.J., Jakobsen, J.S., Karzynski, M.M., Eichenlaub, M.P., Bork, P., and Furlong, E.E. (2006). A temporal map of transcription factor activity: mef2 directly regulates target genes at all stages of muscle development. Dev. Cell *10*, 797–807.
26. Henderson, S.A., Spencer, M., Sen, A., Kumar, C., Siddiqui, M.A., and Chien, K.R. (1989). Structure, organization, and expression of the rat cardiac myosin light chain-2 gene. Identification of a 250-base pair fragment which confers cardiac-specific expression. J. Biol. Chem. *264*, 18142–18148.
27. Richard, I., Roudaut, C., Fougerousse, F., Chiannilkulchai, N., and Beckmann, J.S. (1995). An STS map of the limb girdle muscular dystrophy type 2A region. Mamm. Genome *6*, 754–756.
28. Liu, W., Pajusalu, S., Lake, N.J., Zhou, G., Ioannidis, N., Mittal, P., Johnson, N.E., Weihl, C.C., Williams, B.A., Albrecht, D.E., et al. (2019). Estimating prevalence for limb-girdle muscular dystrophy based on public sequencing databases. Genet. Med. *21*, 2512–2520.
29. Ojima, K., Ono, Y., Ottenheijm, C., Hata, S., Suzuki, H., Granzier, H., and Sorimachi, H. (2011). Non-proteolytic functions of calpain-3 in sarcoplasmic reticulum in skeletal muscles. J. Mol. Biol. *407*, 439–449.
30. Dayanithi, G., Richard, I., Viero, C., Mazuc, E., Mallie, S., Valmier, J., Bourg, N., Herasse, M., Marty, I., Lefranc, G., et al. (2009). Alteration of sarcoplasmic reticulum ca release in skeletal muscle from calpain 3-deficient mice. Int. J. Cell Biol. *2009*, 340346.
31. Lawal, T.A., Wires, E.S., Terry, N.L., Dowling, J.J., and Todd, J.J. (2020). Preclinical model systems of ryanodine receptor 1-related myopathies

and malignant hyperthermia: a comprehensive scoping review of works published 1990-2019. Orphanet J. Rare Dis. *15*, 113.

32. Frey, J.L., Kim, S.P., Li, Z., Wolfgang, M.J., and Riddle, R.C. (2018). β-Catenin Directs Long-Chain Fatty Acid Catabolism in the Osteoblasts of Male Mice. Endocrinology *159*, 272–284.
33. Tribulo, P., Leão, B.C.D.S., Lehloenya, K.C., Mingoti, G.Z., and Hansen, P.J. (2017). Consequences of endogenous and exogenous WNT signaling for development of the preimplantation bovine embryo. Biol. Reprod. *96*, 1129–1141.
34. Ackers, I., and Malgor, R. (2018). Interrelationship of canonical and non-canonical Wnt signalling pathways in chronic metabolic diseases. Diab. Vasc. Dis. Res. *15*, 3–13.
35. Jaka, O., Casas-Fraile, L., Azpitarte, M., Aiastui, A., López de Munain, A., and Sáenz, A. (2017). FRZB and melusin, overexpressed in LGMD2A, regulate integrin β1D isoform replacement altering myoblast fusion and the integrin-signalling pathway. Expert Rev. Mol. Med. *19*, e2.
36. Kohn, A.D., and Moon, R.T. (2005). Wnt and calcium signaling: beta-catenin-independent pathways. Cell Calcium *38*, 439–446.
37. McQuate, A., Latorre-Esteves, E., and Barria, A. (2017). A Wnt/Calcium Signaling Cascade Regulates Neuronal Excitability and Trafficking of NMDARs. Cell Rep. *21*, 60–69.
38. von Maltzahn, J., Chang, N.C., Bentzinger, C.F., and Rudnicki, M.A. (2012). Wnt signaling in myogenesis. Trends Cell Biol. *22*, 602–609.
39. von Maltzahn, J., Bentzinger, C.F., and Rudnicki, M.A. (2011). Wnt7a-Fzd7 signalling directly activates the Akt/mTOR anabolic growth pathway in skeletal muscle. Nat. Cell Biol. *14*, 186–191.
40. von Maltzahn, J., Renaud, J.M., Parise, G., and Rudnicki, M.A. (2012). Wnt7a treatment ameliorates muscular dystrophy. Proc. Natl. Acad. Sci. USA *109*, 20614–20619.
41. Werner, M., Del Castillo, U., Ventrella, R., Brotslaw, E., and Mitchell, B. (2018). The small molecule AMBMP disrupts microtubule growth, ciliogenesis, cell polarity, and cell migration. Cytoskeleton (Hoboken) *75*, 450–457.
42. Tríbulo, P., Bernal Ballesteros, B.H., Ruiz, A., Tríbulo, A., Tríbulo, R.J., Tríbulo, H.E., Bo, G.A., and Hansen, P.J. (2017). Consequences of exposure of embryos produced in vitro in a serum-containing medium to dickkopf-related protein 1 and colony stimulating factor 2 on blastocyst yield, pregnancy rate, and birth weight. J. Anim. Sci. *95*, 4407–4412.
43. Tribulo, P., Moss, J.I., Ozawa, M., Jiang, Z., Tian, X.C., and Hansen, P.J. (2017). WNT regulation of embryonic development likely involves pathways independent of nuclear CTNNB1. Reproduction *153*, 405–419.
44. Ermolova, N., Kudryashova, E., DiFranco, M., Vergara, J., Kramerova, I., and Spencer, M.J. (2011). Pathogenity of some limb girdle muscular dystrophy mutations can result from reduced anchorage to myofibrils and altered stability of calpain 3. Hum. Mol. Genet. *20*, 3331–3345.
45. Nadaj-Pakleza, A.A., Dorobek, M., Nestorowicz, K., Ryniewicz, B., Szmidt-Sałkowska, E., and Kamińska, A.M. (2013). Muscle pathology in 31 patients with calpain 3 gene mutations. Neurol. Neurochir. Pol. *47*, 214–222.
46. Kramerova, I., Kudryashova, E., Wu, B., and Spencer, M.J. (2006). Regulation of the M-cadherin-beta-catenin complex by calpain 3 during terminal stages of myogenic differentiation. Mol. Cell. Biol. *26*, 8437–8447.
47. Acin-Perez, R., Benador, I.Y., Petcherski, A., Veliova, M., Benavides, G.A., Lagarrigue, S., Caudal, A., Vergnes, L., Murphy, A.N., Karamanlidis, G., et al. (2020). A novel approach to measure mitochondrial respiration in frozen biological samples. EMBO J. *39*, e104073.

STAR★METHODS

KEY RESOURCES TABLE

REAGENT or RESOURCE	SOURCE	IDENTIFIER
Antibodies		
Mouse monoclonal anti-CaMKIIβ	Thermo Fisher Scientific	Cat# 13-9800; RRID:AB_2533045
Mouse monoclonal anti-phospho-CaMKII (22B1)	Thermo Fisher Scientific	Cat# MA1-047; RRID:AB_325402
Rabbit polyclonal anti-Akt	Cell Signaling	Cat# 9272; RRID:AB_329827
Rabbit polyclonal anti-phospho Ser473-Akt	Cell Signaling	Cat# 9271; RRID:AB_329825
Rabbit polyclonal anti-phospho Thr308-Akt	Cell Signaling	Cat# 9275; RRID:AB_329825
Rabbit polyclonal anti-AMPK	Cell Signaling	Cat# 2532; RRID:AB_330331
Anti-phospho Thr172-AMPK	Cell Signaling	Cat# 4188; RRID:AB_2169396
Mouse monoclonal anti-slow myosin heavy chain	Leica Microsystems	Cat# NCL-MHCs; RRID:AB_563898
Mouse monoclonal anti-fast myosin heavy chain	Leica Microsystems	Cat# NCL-MHCf; RRID:AB_563899
Rabbit polyclonal anti-laminin	Sigma	Cat# L9393; RRID:AB_477163
Bacterial and Virus Strains		
Top10 Chemically Competent E.coli	Thermo Fisher Scientific	Cat# C404010
Chemicals, Peptides, and Recombinant Proteins		
Prestwick library of small molecules	Microsource	Spectrum Collection
LOPAC library of small molecules	Sigma	Cat# LOPAC-1280
AMBMP	R&D system	Cat# 6043
Lansoprazole	Sigma	Cat# L8533
Rabeprazole	Abcam	Cat# Ab143690
Parbendazole	Sigma	Cat# 32438
Nitro Blue Tetrazolium	Sigma	Cat# N6876
Reduced NADH	Sigma	Cat# N8129
Geneticin	ThermoFisher Scientific	Cat# 11811031
Trizol	ThermoFisher Scientific	Cat# 15596018
iTaq Universal SYBR Green Supermix	Bio-Rad	Cat# 1725124
propidium iodide (PI)	ThermoFisher Scientific	Cat# P3566
Hoescht 33342	ThermoFisher Scientific	Cat# H3570
Fetal Bovine Serum	ThermoFisher Scientific	Cat# 10082147
Horse Serum	ThermoFisher Scientific	Cat# 26050088
DMEM	ThermoFisher Scientific	Cat# 11965092
Collagenase Type II	Worthington	Cat# LS004177
Insulin-Transferrin-Selenium-Ethanolamine (ITS-X)	ThermoFisher Scientific	Cat# 51500056
Protease and Phosphatase Inhibitor Cocktail	ThermoFisher Scientific	Cat# 78441
Protease Inhibitor Cocktail	Sigma	Cat# P8340
DMSO	Sigma	Cat# D2438
ViaFect Transfection Reagent	Promega	Cat# E4981
Ponceau S Red	Sigma	Cat# P7170
iScript Reverse Transcriptase Supermix	Bio-Rad	Cat. No.: 1708841
Critical Commercial Assays		
Bright-Glo luciferase kit	Promega	Cat. No. E2620
CellTiter-Glo® Viability Assay	Promega	Cat. No. G9242
Experimental Models: Cell Lines		
C2C12 cell line	ATCC	RRID:CVCL_UR38

(*Continued on next page*)

Continued

REAGENT or RESOURCE	SOURCE	IDENTIFIER
WT (C57 BL/6J) primary myoblast cell line	This paper	N/A
C3KO (CAPN3 knockout) myoblast cell line	This paper	N/A
Experimental Models: Organisms/Strains		
Mouse: C57BL/6J	Jackson Laboratories	RRID:IMSR_JAX:000664
Mouse: CAPN3 knockout, C3KO	[10]	N/A
Oligonucleotides		
RT-PCR Gapdh forward 5′- GACTTCAACAGCAACTCCCAC-3′	This paper	N/A
RT-PCR Gapdh reverse 5′- TCCACCACCCTGTTGCTGTA-3′	This paper	N/A
RT-PCR Myl2 forward 5′- AGTTCAAGGAAGCCTTCACAATC-3′	This paper	N/A
RT-PCR Myl2 reverse 5′- ATTGGACCTGGAGCCTCTTTGAT-3′	This paper	N/A
RT-PCR Ckmt2 forward 5′- ATAGGCAGAAGGTATCTGCTGATG-3′	This paper	N/A
RT-PCR Ckmt2 reverse 5′- GTGTCATCTTGTTTCGGAGTTTGG-3′	This paper	N/A
RT-PCR Pnpla2 forward 5′- CTCACATCTACGGAGCCTCG	This paper	N/A
RT-PCR Pnpla2 reverse 5′-CCAGGTTGAAGGAGGGATGC	This paper	N/A
RT-PCR Camk2b forward 5′ CAGATGGAGTCAAGCCCCAG	This paper	N/A
RT-PCR Camk2b reverse 5′ TTGTGTTGGTGCTGTCGGAA	This paper	N/A
Recombinant DNA		
pGL4.17	Promega	E672A
Plasmid: 1 kb *Myl2* promoter in pGL4.17	This paper	N/A
Plasmid: 3 kb *Myl2* promoter in pGL4.17	This paper	N/A
Software and Algorithms		
Axio Vision software	Zeiss	N/A

RESOURCE AVAILABILITY

Lead Contact

Further information and requests for resources and reagents should be directed to and will be fulfilled by the Lead Contact, Melissa J. Spencer (mspencer@mednet.ucla.edu).

Materials Availability

This study generated new plasmid constructs that are available upon request without restriction.

Data and Code Availability

This study did not generate new datasets that have not been previously published in scientific literature.

EXPERIMENTAL MODEL AND SUBJECT DETAILS

Mouse Models

Animal husbandry and veterinary care was provided by the Department of Laboratory Animal Medicine at University of California, Los Angeles (UCLA). Experimental procedures were reviewed and approved by UCLA Research Safety and Animal Welfare Administration.

Adult male mice (5-7 month old) were used in all studies except primary cell isolation, for which 14 day old pups (both males and females) were used. Calpain 3 KO (C3KO) mice were described previously.[10] C57 BL/6J mice were obtained from the Jackson Laboratories. Animals were maintained in a pathogen-free animal facility under 12hr light/12hr dark cycle with access to a standard rodent chow and water *ad libitum*.

Cell lines used

The C2C12 cell line was obtained from ATCC. C2C12 cells were cultured in DMEM medium supplemented with 10% FBS (growth medium). For differentiation, C2C12 cells were cultured in growth media for 2 days and then switched to differentiation media

(DMEM + 2% horse serum). The media was replaced with fresh differentiation media every day for 6 days (D0 to D6) until the myotubes were fully developed.

METHOD DETAILS

Animal studies

For the run to exhaustion experiment, mice were run at 10 m/min for the first 10 min (0-10 min), at 12 m/min during 10-30 min and 14 m/min during 30-60 min. After 60 min, the speed was increased by 2 m/min every 5 min until the mouse was unable to continue. All mice used for these experiments were males (n = 6 per group for each genotype), aged 5-6 months.

Treatment of C2C12 cells

For compound treatment, C2C12 cells were seeded at a density of 30,000 cells/well in 24 well plates in growth medium. Twenty-four hours later, the medium was changed to differentiation medium and compounds were added at different concentrations. Forty-eight hours later, cells were harvested for RNA extraction and qPCR analysis.

Cloning of Myl2 promoter reporter constructs and generation of C2C12 stable cell lines

We amplified 1 and 3 kb fragments of the *Myl2* promoter from genomic DNA isolated from mouse myoblasts. These promoter fragments were cloned into XhoI/BglII sites of the pGL4.17 vector upstream of firefly luciferase. The resulting constructs were transfected into C2C12 cells and selected with G418 (850 ug/ml) for two weeks to generate stable cell lines.

High throughput and secondary screening

Stably transfected C2C12 cells were seeded at a density of 4,000 cells/well into 384 well plates in myoblast growth medium. Medium was changed to differentiation medium after 24 hours and then the compound library was added to the cells. Both the Prestwick and LOPAC libraries were screened. In the initial screen, all the compounds were added at 10 μM with a final concentration of 1% DMSO. Each compound was tested in a single well. Forty-eight hours later, cells were lysed, and luciferase activity was measured with Bright-Glo luciferase kit (Promega). Primary hits were defined as compounds that produced an increase in luciferase activity of more than 3 standard deviations over vehicle (DMSO) control wells (z score = 3). The Z score was calculated based on this formula: $z\ score = (sample - Neg.\ Ctrl.\ Mean\ /StDev\ of\ Neg.\ Ctrl.)$ The hits identified from initial screening were further verified in triplicate in secondary screening.

Compound dose response analysis

C2C12 stable cells were plated in 384 well plates in myoblast culture media at 4,000 cells per well density. Twenty-four hours later, medium was switched to differential medium and each compound was added to cells over a range of concentrations (0 to 100 μM). Luciferase reporter activity was measured after 48 hr.

Cytotoxicity and viability assay

The cytotoxicity and cell viability of compounds was analyzed by propidium iodide (PI)/ Hoescht 33342 staining and CellTiter-Glo® Viability Assay, respectively. Briefly, C2C12 cells were seeded in 384-well plates at 4,000 cells per well and compounds were added in a 20-point dose titration (from 0.0002-100 μM). Forty-eight hours later, PI and Hoescht 33342 were added at 5 μM and 5 μg/ml final concentration. Plates were incubated at room temperature for 1 hr and then images were taken with MicroXpress. For CellTiter-Glo assay, 48 hr after compound treatment, lysis solution was added to each well at volume 1:1 ratio and the luciferase activity was measured using a plate reader (Perkin Elmer).

Compound treatment of C2C12 cells

For compound treatment, C2C12 cells were seeded at a density of 30,000 cells/well in 24 well plates in growth medium. Twenty-four hours later, the medium was changed to differentiation medium and compounds were added at different concentrations. Forty-eight hours later, cells were harvested for RNA extraction and qPCR analysis.

Isolation and compound treatment of primary myoblasts

Hind limbs of 14-day old mouse pups (both WT and C3KO) were dissected and primary myoblasts were isolated using collagenase/dispase digestion, as described before.[46] Myoblasts were used for experiments for no longer than 10 passages. Primary myoblasts were differentiated in 2% HS differentiation medium as described for C2C12 cells. For compound treatment, 70,000 primary cells per well were seeded into 12-well plates in growth media. Medium was changed to differentiation media 24 h after seeding and the compounds were added to the differentiating myotubes. Cells were harvested for qPCR analysis after 48 h of treatment.

Real-time PCR

Total RNAs were isolated from cells or tissues using Trizol. cDNA was generated using iScript Reverse Transcriptase Supermix (Bio-Rad) and was used for real-time PCR with iTaq Universal SYBR Green Supermix (BioRad) according to the manufacturer's

instructions. All real-time PCR reactions were run in CFX Connect Real-Time PCR System (Bio-Rad). The primers used in these experiments are shown in the Key Resources Table.

Compound pharmacokinetics assay

For pharmacokinetics, AMBMP was administered by different routes of delivery (subcutaneous, intraperitoneal, and oral, in food or by gavage) at two different dosages (10 mg/kg and 30 mg/kg). The blood was collected at 0.5 h, 1 h, 2 h, 4 h and 6 h post treatment by heart puncture. The concentrations of compounds in plasma were analyzed by Integrated Analytical Solutions, Inc.

Quantification of cross-sectional area and NADH staining

Soleus muscles were isolated from control and compound treated mice and frozen in OCT. The frozen samples were sectioned and stained for slow or fast isoforms of myosin heavy chain (both antibodies were from Novocastra). The cross-sectional area (CSA) was quantified on slow and fast fibers separately using Axio Vision software (Zeiss).

For NADH staining, plantaris frozen sections were air-dried at room temperature and then incubated with staining solution (50 mM Tris-HCl, pH7.4 + 1mg/ml Nitro Blue Tetrazolium and 1 mg/ml reduced NADH) at 37C for 1 hr. All reagents were from Sigma. After incubation, slides were washed quickly in 30%, 60%, 90%, 60%, 30% acetone and in water. NADH histochemistry leads to three distinguishable levels of staining that we identified as low, intermediate and high. The three levels of staining were analyzed blindly to ensure objectivity. We refer to the low stained fiber as fast glycolytic (FG), and the intermediate plus high together as fast glycolytic/oxidative (FOG).

Seahorse analysis of Extracts from Frozen Muscle

For Seahorse analysis, frozen soleus muscles from DMSO or AMBMP-treated mice (daily IP injections at 7.5 mg/kg) were homogenized by hand in a Dounce homogenizer in 200 mL of mitochondrial buffer (70 mM sucrose, 220 mM mannitol, 5 mM KH_2PO_4, 5 mM $MgCl_2$, 1 mM EGTA, 2 mM HEPES, adjusted to pH 7.4 with KOH) on ice. Muscle homogenates were centrifuged at 900xg for 5 min at 4°C. Supernatants were transferred to new tubes; protein concentrations were measured using BCA protein Assay Kit (Thermo Fisher Scientific). The samples (4 μg/well) were analyzed in the UCLA Mitochondrial and Metabolism Core using a Seahorse XF96 Analyzer (Agilent). Data were normalized to total protein. Seahorse analysis was carried out according to Acin-Perez et al.[47]

Western blot analysis

Muscles were homogenized by hand in a Dounce homogenizer in reducing sample buffer (80 mM Tris, pH 6.8, 10% β-Mercaptoethanol, 2% SDS and 10% glycerol) with phosphatase inhibitor (Thermo scientific) and protease inhibitor cocktail (Sigma). An equal amount of total protein was loaded on SDS-PAGE gels followed by transfer to nitrocellulose membrane. Ponceau red S was used to verify the transfer onto the nitrocellulose. The following primary antibodies were used for western blotting: anti- β-CaMKII (1:500, Life Technologies), anti- phospho-CaMKII (1:750, Thermo Scientific), anti-AMPK (1:1000), anti-phospho (T172) AMPK (1:1000), anti-Akt (1:1000), anti-phospho Akt (1:500)(Cell Signaling). Secondary antibodies conjugated with HRP were from Sigma-Aldrich (used 1:10000). Specific signals were developed using ChemiGlow chemiluminescent substrate for HRP (Protein Simple). Images of the blots were acquired using FluorChem FC2 Imager (Alpha Innotech). Specific signals were developed using ChemiGlow chemiluminescent substrate for HRP (Protein Simple). Images of the blots were acquired using FluorChem FC2 Imager (Alpha Innotech). Quantitative analysis was performed using ImageJ software.

Statistical analysis

For all studies, results from quantitative experiments were expressed as means ± SEM and were analyzed using Prism (GraphPad) software. Where appropriate, significance was calculated by Student's t test, one-way ANOVA with Tukey's multiple comparison post hoc analysis. Exact p values are listed in the figures. A p value less than 0.05 was considered statistically significant.